Contribution from Ames Laboratory[1] and the Department of Chemistry, Iowa State University, Ames, Iowa 50011

# Structure of the Intermediate $Zr_2Br_2H$ by Neutron Diffraction and Its Structural and Bonding Relationships to Other Phases

Sunil D. Wijeyesekera and John D. Corbett*

*Received May 29, 1986*

The structures of the isomorphous $Zr_2Br_2D$ and $Zr_2Br_2H$ have been solved and refined by using Rietveld techniques on pulsed neutron diffraction data obtained from the powdered samples at 14 K ($C2/m$, $a$ = 19.437 (3) Å, $b$ = 3.5253 (4) Å, $c$ = 5.9036 (6) Å, $\beta$ = 100.98 (1)°, $R$(profile)/$R$(expected) = 2.44 for the deuteride). The structure consists of layers sequenced Br–Zr–H–H–Zr–Br and arranged such that hydride lies in zigzag chains of distorted metal tetrahedra (or butterflies) ($d$(Zr–D) = 2.03–2.20 Å; $d$(D–D) = 2.93 Å). The structure is intermediate between ZrBr (ccp) and ZrBrH (hcp heavy atoms, double H in trigonal-antiprismatic interstices) and can be generated by concerted intraslab slippage from either. The hemihydride effectively retains most of the strong Zr–Zr bonding of the ZrBr parent while tetrahedral bonding of hydrogen to metal is gained that is absent in ZrBrH. The energetics associated with the contrasting structures of $YClH_x$ (ZrBr type) and ZrBrH are considered in terms of the results of extended-Hückel band calculations.

## Introduction

The metallic compounds ZrCl and ZrBr[2] show particularly unusual and interesting reactions with hydrogen. Although these proceed even at room temperature, the reactions are faster and the crystallinity of the products is better at 250–400 °C. Measurements of hydrogen dissociation pressures demonstrate that two consecutive two-phase equilibria occur, the first between the parent monohalide and a hemihydride, $Zr_2X_2H$, and the second between that hydride and the monohydride ZrXH (X = Cl, Br).[3] Both hydrides exhibit some compositional breadth at elevated temperatures, but high-precision Guinier powder data indicate that they are essentially line phases at room temperature. The hydrogen pressure data for equilibria between pairs of the halide hydrides yield enthalpy changes that are about 60% as large as that for the formation of $ZrH_{1.5}$.

The structures of the initial ZrX matrix and of the product hydrides demonstrate the unusual character of these transformations. The host structures contain strongly bonded slabs that consist of four close-packed layers sequenced X–Zr–Zr–X and ordered AbcA (upper case letters denote the relative orientation of the halogen layers and lower case letters the relative orientation of the metals).[4] The distinction between ZrCl and ZrBr structures occurs only in the stacking order of these weakly bound slabs in a rhombohedral cell.[5] The thermochemical characterization of the hydride reactions and their ready reversibility suggest that the character of the basic structure is retained and that the hydrogen is bonded in the somewhat compressed polyhedra between the double-metal layers. It was noted early on that $Zr_2X_2H$ and ZrXH stoichiometrically correspond to the occupation of all octahedral and all tetrahedral cavities, respectively, between the double-metal layers.[3] Not only is this order of filling somewhat unusual, but it is also just the reverse of the interstices actually utilized at each stage.

The location of the heavy atoms in the hydride structures was first approximated by refinement of X-ray powder data for $Zr_2Br_2H$ and ZrXH (X = Cl, Br) which showed that the sequence of layers is retained in the two structures but with altered ordering in projection.[6] Each cubic-close-packed slab in ZrX (AbcA) rearranges to a hexagonal-close-packed (AbaB) one in the trigonal ZrXH ($P\bar{3}m1$) while $Zr_2Br_2H$ appears to represent an approximate midpoint between these two with only monoclinic ($C2/m$) symmetry. Equivalent sections of these three structures are shown in Figure 1 where it can be seen that the progressive displacement of the upper pair of Br and Zr layers carries the ZrBr arrangement first into that in $Zr_2Br_2H$ and then to ZrBrH. However, the nonequivalent sites for hydrogen that would be necessary in the intermediate to achieve the hemihydride stoichiometry could not be distinguished. ($Zr_2Cl_2H$ presumably has a very similar structure, but the different unit cell arising because of the alternate slab sequence in ZrCl has not been uncovered.)

The position of hydrogen in these structures is, of course, particularly important. Its probable location in tetrahedral-like interstices between the double-metal layers has been indicated by several NMR studies,[7-9] especially by the magnitudes of the anisotropic shielding and the observed proton second moments. This configuration would correspond to complete occupation of the tetrahedral sites between the double-metal layers in the monohydride and half in the hemihydride, although detailed agreement with second-moment calculations for a rigid lattice required some small occupation of octahedral sites as well. The probable presence of zig-zag chains of occupied tetrahedra in the hemihydride was inferred from the beginning on the basis of the magnitude of the dominant proton–proton coupling, the need for reasonable H–H distances, and the stoichiometry.[7] Knowledge of the X-ray (heavy-atom) structure of $Zr_2Br_2H$ has led to a detailed analysis of the two-step motional narrowing of the NMR lines in terms of dominant tetrahedral and minor octahedral site occupancies.[9]

The details of this intermediate structure became all the more intriguing when our recent pulsed neutron study[10] showed that ZrBrD (and presumably the isostructural ZrClH) involved the placement of deuterium not in separate tetrahedral but in pairs near opposed faces of all trigonal antiprisms ("octahedra") defined by the double-metal layers. These locations are marked with solid dots in Figure 1c. This double occupancy occurs here in antiprisms that have no halogen neighbors along $z$, a configuration that was created by the rearrangement of the ZrX structure (Figure 1). The neutron data refinement indicated a small but nonzero occupancy of the nominally vacant $Zr_4$ tetrahedra in ZrBrD was also probable at room temperature.

The present study reports on a neutron diffraction study at the Intense Pulse Neutron Source (IPNS) at Argonne National Laboratory of the polycrystalline $Zr_2Br_2D$ and, in later clarification, $Zr_2Br_2H$ together with further definition of the interrelationships implied by the X-ray results shown in Figure 1. Both measurements were made at 14 K both in recognition of the fact that two steps of line narrowing arising from proton motion could be clearly seen in the NMR data for this compound at about 170

(1) This research was supported by the Office of Basic Energy Sciences, Materials Sciences Division. Ames Laboratory is operated for the U.S. Department of Energy by Iowa State University under Contract No. W-7405-Eng-82.

(2) Struss, A. W.; Corbett, J. D. *Inorg. Chem.* **1970**, *9*, 1373.
(3) Struss, A. W.; Corbett, J. D. *Inorg. Chem.* **1977**, *16*, 360.
(4) Adolphson, D. G.; Corbett, J. D. *Inorg. Chem.* **1976**, *15*, 1820.
(5) Daake, R. L.; Corbett, J. D. *Inorg. Chem.* **1977**, *16*, 2029.
(6) Marek, H. S.; Corbett, J. D. Daake, R. L. *J. Less-Common Met.* **1983**, *89*, 243.
(7) Hwang, T. Y.; Torgeson, D. R.; Barnes, R. G. *Phys. Lett. A* **1978**, *66A*, 137.
(8) Murphy, P. D.; Gerstein, B. C. *J. Chem. Phys.* **1979**, *70*, 4552.
(9) Hwang, T. Y.; Schoenberger, R. J.; Torgeson, D. R.; Barnes, R. G. *Phys. Rev. B: Condens. Matter* **1983**, *27*, 27.
(10) Wijeyesekera, S. D.; Corbett, J. D. *Solid State Commun.* **1985**, *54*, 657.

0020-1669/86/1325-4709$01.50/0 

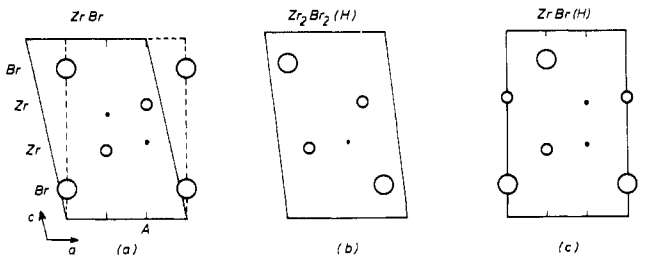


**Figure 1.** Sections of one slab of the structures of (a) ZrBr ($YClH_x$), (b) $Zr_2Br_2H$, and (c) ZrBrH (these are shown in the common space group or subgroup $C2/m$ with the $c$ axis vertical and the layers horizontal): large circles, bromine; small circles, zirconium; solid dots, hydrogen in particular cases (see text).

and 260 K[9] and in order to maximize the likelihood of good hydrogen order both in space and in time, especially between the weakly interacting slabs. The new diffraction results further highlight the contrasting behavior of the neighboring yttrium where YCl does not exist, while hydrogen in the known phase $YClH_x$, $\sim 0.6 < x < \sim 1.0$, apparently occurs in tetrahedral sites in a basically unchanged ZrBr-type matrix,[11,12] analogous to the behavior of $TbClD_{0.8}$[13] and in contrast to the rearrangements described above for zirconium. Some results of extended-Hückel calculations are also provided in clarification of both the unusual structural contrast between YClH and ZrXH and the instability of the $d^2$ YCl relative to $d^3$ ZrCl.

## Experimental Section

**Diffraction Experiments.** The syntheses of $Zr_2Br_2D$ and $Zr_2Br_2H$ were carried out as before.[6] Time-of-flight neutron diffraction data were collected on the special environment powder diffractometer at the IPNS at Argonne National Laboratory.[14,15] Data from 4 g of the deuteride sealed in a vanadium container were collected for 18 h at 14 K and, later, from 5 g of the hydride for 30 h at the same temperature. Good statistics were obtained with the former data set at $2\theta = 90°$ while those from the hydride were not nearly as good in spite of the larger quantity and longer time, evidently because the larger incoherent scattering length of hydrogen resulted in a much lower signal-to-noise ratio. A five-parameter-shifted Chebyshev polynomial was used in the latter case for background removal instead of the usual two-parameter exponential.

**Models and Refinement.** The heavy-atom structure of $Zr_2Br_2H(D)$ deduced by X-ray diffraction is represented in Figure 1b by its [010] section. In this case the next layer at $y = {}^1/_2$ is generated by a C-centering operation that is in effect comparable to the replication found with close-packed structures.

Three regular ways of distributing hydrogen among half of the (distorted) tetrahedral sites available between the double-metal layers can be conceived of without an increase in cell dimensions, all utilizing subgroups of the parent $C2/m$. These are shown in Figure 2 in views normal to the slabs: (a) pairs of hydrogen in tetrahedral interstices sharing edges ($P2/m$); (b) zig-zag chains of $Zr_4H$ tetrahedra along $b$ ($P2_1/m$); and (c) two-dimensional layers of hydrogen (all up or all down and therefore polar) ($Cm$). For each of these there are two simple ways to order hydrogen in adjacent slabs, either the same (AA) or opposed (AB), the latter doubling the $c$ axis that lies more-or-less normal to the layers shown. A random hydrogen distribution can also be considered, either because there is no long-range order within a slab or because an interlayer regularity does not exist at 14 K.

All seven models were refined by Rietveld methods for $Zr_2Br_2D$ and five proceeded smoothly to give virtually identical $R$ values: $R$(profile)/$R$(expected limit) = 2.43–2.49; $R$(weighted profile)/$R$(expected) = 3.57–3.76.[16] Only models (b)(AA) and (c)(AA) were eliminated in this process. However, two more that involve pairs of atoms, (a)(AA) and (a)(AB), could logically be discarded since their refinement yielded D–D distances, 1.90 (2) and 2.01 (2) Å, respectively, that were unreasonably short on the basis of both our knowledge of other structures and empirical hydride radii.[17–19] There were thus three possible models remaining: (b)(AB), zig-zag; (c)(AB), layers; and (AA), random. Lack of resolution among these presumably occurs not only because of similar nuclear density maps for the heavy atoms and comparable site symmetries for the deuterium occur in all but also because in every case the refinement to minimize $R$ causes compensating movement of the heavy atoms. Although none of these shifts produces results that would lead to rejection of that model, they are sufficient to make the results ambiguous. The extra reflections that originate from the supercell in the first two of the remaining models turn out to have less than 5% of the maximum observed intensity and are lost in the background at the higher $d$ values where they might be identified. Furthermore, the expected intensity differences among the remaining low-angle reflections for the three models are very small, as shown in Table I.

**Table I.** Calculated Neutron Diffraction Intensities for Three Different Models of $Zr_2Br_2D$[a]

| | two slab | | |
|---|---|---|---|
| $d$, Å | zigzag | layers | random |
| 2.932 | 123 | 129 | 135 |
| 2.930 | 102 | 96 | 96 |
| 2.833 | 109 | 110 | 113 |
| 2.793 | | 55 | |
| 2.717 | 91 | 97 | 102 |
| 2.636 | 172 | 186 | 190 |
| 2.623 | 1000 | 1000 | 1000 |
| 2.487 | 166 | 175 | 168 |
| 2.385 | 288 | 300 | 298 |
| 2.379 | 320 | 319 | 317 |
| 2.129 | 134 | 148 | 141 |
| 2.042 | 124 | 123 | 128 |
| 1.963 | 148 | 154 | 151 |
| 1.928 | 101 | 99 | 97 |
| 1.908 | 141 | 150 | 152 |
| 1.821 | 205 | 195 | 202 |
| 1.763 | 342 | 347 | 349 |
| 1.712 | 247 | 257 | 269 |
| 1.709 | 154 | 155 | 141 |
| 1.663 | 184 | 188 | 193 |
| 1.654 | 154 | 154 | 144 |
| 1.522 | 54 | 55 | 63 |
| 1.511 | 62 | 67 | 68 |

[a] Maximum = 1000.

The resolution of this ambiguity was accomplished by collecting data on the hydride $Zr_2Br_2H$ since the coherent scattering lengths of D and H are so different, 0.67 and $-0.372 \times 10^{-14}$ m, respectively. Clearly the deuteride and hydride must have the same structure as well as virtually the same bond lengths and angles. Because of the poorer statistics in the hydride data set (above), the atom positions for each of the three models were constrained to the refined values found with the deuteride, and only ten parameters were thus varied: scale, absorption, extinction, and two profile together with the five describing the background. Since we have perturbed the scattering lengths by using hydrogen, much larger differences between structures appear in the $R$ values. The hydride refinement clearly identifies the alternating zig-zag chain model, (b)(AB), to be the correct one, with $R_p/R_e = 3.00$ and $R_{wp}/R_e = 4.02$ vs. 3.22 and 4.26 for (c)(AB) and 3.45 and 4.95 for the random distribution.

The final refinement of the $Zr_2Br_2D$ structure with the zig-zag chains of Figure 2b and the deuterium in the adjacent slab out of phase varied 25 parameters: scale, two background, six profile, four cell, one extinction, ten positional, and the thermal parameter for D. The effect of preferred orientation, often a serious matter with these platelike crystallites, is dealt with approximately in the available programs by means of a Gaussian distribution about a specified preferred orientation direction. This correction was observed to make a significant difference with ZrBrD,[10] but here it refined to 0.36 for $Zr_2Br_2D$, almost twice the value found before. The physical significance of this was not felt to be convincing, and so the parameter was fixed at 0.25. Although this made $R_p$ very slightly larger, $R(F^2)$ decreased 10%.

There was also a tendency with all three models for the thermal parameter of at least one of the heavy atoms to refine to a negative value.

(11) Wijeyesekera, S. D.; Corbett, J. D., unpublished research.
(12) Mattausch, Hj.; Eger, R.; Simon, A., unpublished research.
(13) Ueno, F.; Ziebeck, K.; Mattausch, Hj.; Simon, A. *Rev. Chim. Miner.* **1984**, *21*, 804.
(14) Jorgensen, J. D.; Rotella, F. J. *J. Appl. Crystallogr.* **1982**, *15*, 27.
(15) Von Dreele, R. B.; Jorgenson, J. D.; Windsor, C. G. *J. Appl. Crystallogr.* **1982**, *15*, 581.
(16) The number of scans enters into the definitions of all $R$ values, and therefore quotients of observed to the theoretical $R$ limits are more meaningful. Values of 3.0 or less for $R$(profile)/$R$(expected) are considered acceptable.
(17) Corbett, J. D.; Marek, H. S. *Inorg. Chem.* **1983**, *22*, 3194.
(18) Westlake, D. G. *J. Less-Common Met.* **1983**, *90*, 251.
(19) The presence of $H_2$ units in such an electron-rich hydride is not consistent with either the hydride valence band revealed by PES studies[17] or the NMR data.[9]

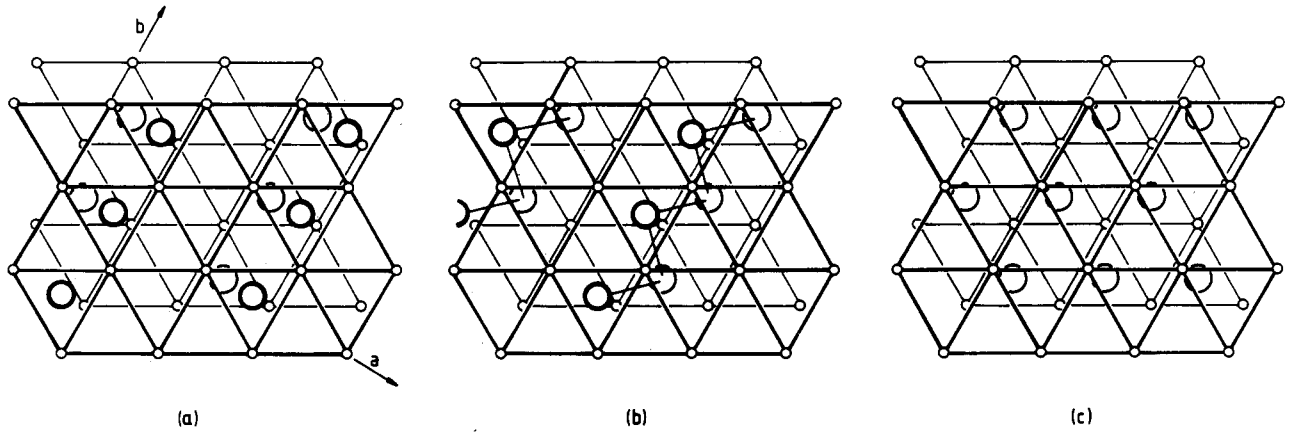


**Figure 2.** Models considered for the $Zr_2Br_2D$ structure viewed normal to the slabs: (a) pairs of deuterium in tetrahedra sharing an edge; (b) zigzag chains of deuterium in tetrahedra sharing corners; (c) two-dimensional layers of deuterium. Small interconnected circles define two layers of zirconium (idealized) with the larger circles between them representing deuterium in metal tetrahedra. (The bromine atoms are not shown.)

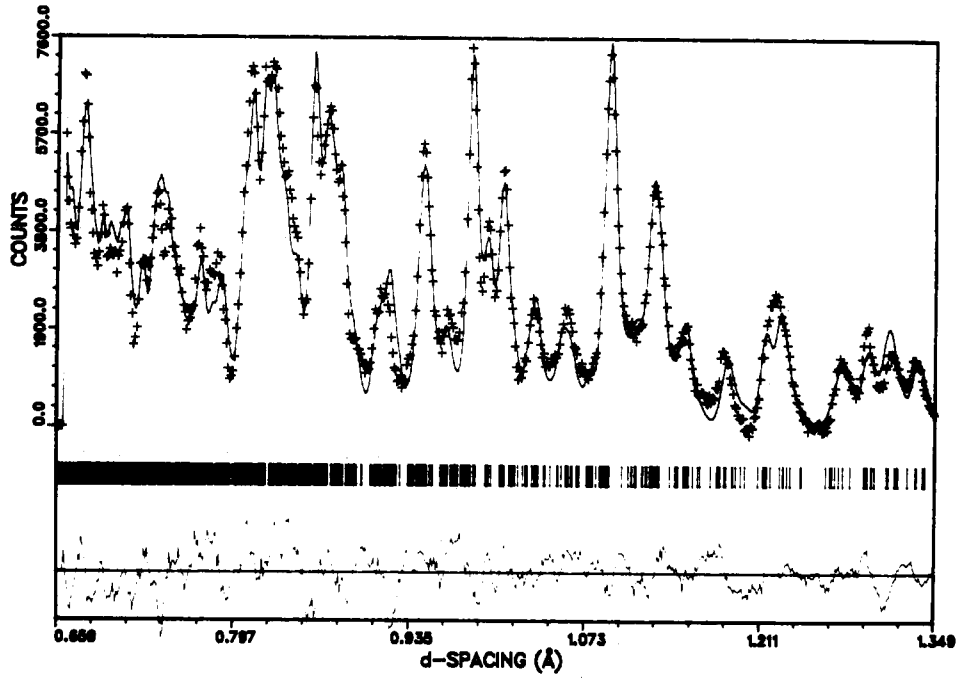


**Figure 3.** Refined pulsed neutron data (14 K, $2\theta = 90°$) for the densest region of the spectrum of $Zr_2Br_2D$: top curve, calculated profile and experimental data (crosses); middle curve, position of reflections included in the fit; bottom curve, observed minus calculated profile.

This was much less serious when preferred orientation and profile parameters were also allowed to refine, the latter being important with stacking disorder (and grinding damage) of the sort that has been observed to be much more serious in related compounds, e.g., in ZrCl[5] and $ZrClO_xD_y$.[11] In the zigzag model, the thermal parameters for the heavy atoms had almost no affect on the $R$'s, and the values obtained were statistically not different from zero, i.e., 0.06 (7) for Zr and −0.19 (7) for Br, and they were therefore fixed at zero. The final $R$ values are close to those obtained for ZrBrD (single site model)[10] while $R(F^2)$ which compares peak intensities is considerably better.

## Results and Discussion

**Structural Results.** The crystal data and atom parameters for $Zr_2Br_2D$ are listed in Table II while the calculated and observed profiles, the $d$ spacings involved, and the difference between the profiles are shown in Figure 3 for the densest region of the spectrum. Distances in the structure are given in Table III. The (AB) orientation of the zigzag chains of deuterium in different slabs and the differentiation of zirconium atoms within the slabs generate a $C$-centered cell with a different angle and with reversed $a$ and $c$ axes relative to those reported from the X-ray study,[6] but the heavy-atom structure is still very close to that in Figure 1b.

The structure of $Zr_2Br_2D$ contains the usual Br–Zr–Zr–Br sequence of infinite layers with a relative placement of the Br–Zr halves such that the adjacent metal layers generate chains of metal

**Table II.** Crystal Data and Atom Parameters for $Zr_2Br_2D$[a]

| Crystal Data | |
|---|---|
| space group | $C2/m$ (monoclinic) |
| $Z$ | 4 |
| $a$, Å | 19.437 (3) |
| $b$, Å | 3.5253 (4) |
| $c$, Å | 5.9036 (6) |
| $\beta$, deg | 100.98 (1) |
| $R$(profile) | 4.06 |
| $R$(weighted profile) | 6.23 |
| $R$({structure factor}$^2$) | 9.24 |
| $R$(expected) | 1.66 |
| $R_p/R_e$ | 2.44 |
| $R_{wt}/R_e$ | 3.75 |

Atomic Parameters[b]

| atom | $x$ | $z$ | $B$,[c] Å$^2$ |
|---|---|---|---|
| Zr(1) | 0.1815 (6) | 0.954 (2) | 0.0 |
| Zr(2) | 0.3154 (6) | 0.547 (2) | 0.0 |
| Br(1) | 0.0851 (6) | 0.221 (2) | 0.0 |
| Br(2) | 0.9168 (7) | 0.283 (2) | 0.0 |
| D | 0.7088 (5) | 0.621 (2) | 0.9 (1) |

[a] Channels = 2100; reflections = 1500, $0.60 < d < 3.2$ Å; $2\theta = 90°$. [b] $y = 0$. [c] See text.

**Table III.** Selected Distances (Å) in $Zr_2Br_2D$ (14 K)

| | | |
|---|---|---|
| Zr(1)–Zr(1) | intralayer | 3.5254 (4) |
| | interlayer | 3.15 (2) |
| Zr(2)–Zr(2) | intralayer | 3.5254 (4) |
| | interlayer | 3.06 (2) |
| Zr(1)–Zr(2) | intralayer (av) | 3.44 (1) |
| | interlayer (av) | 3.90 (1) |
| Zr(1)–Br(av) | | 2.74 (1) |
| Zr(2)–Br(av) | | 2.76 (1) |
| Zr(1)–D | | 2.13 (1) |
| Zr(2)–D | | 2.031 (6) (×2) |
| | | 2.20 (1) |

Shortest Nonbonding Distances

| | |
|---|---|
| Br ··· Br | 3.41 (1) |
| Br ··· D | 3.02 (1) |
| D ··· D | 2.93 (2) |

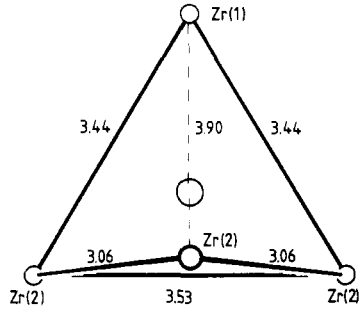


**Figure 4.** The metal tetrahedron enclosing deuterium in the $Zr_2Br_2D$ structure viewed normal to the layers.

polyhedra best described as pairs of distorted tetrahedra that share long (3.90-Å) edges. Deuterium occupies the lesser distorted half of these so as to generate zigzag chains described by a twofold screw axis along *b* (Figure 2b). Simultaneous occupation of the second chain of tetrahedra with only slightly larger dimensions about Zr(2) is precluded by the too close approach of pairs of deuterium atoms (model 2a) and probably by the bromine atoms as well which lie directly above these. Slabs that lie above and below the one shown have the deuterium and zirconium chains reversed, thus doubling the cell in that direction relative to that resolved earlier with X-rays.

The distorted metal tetrahedron and the deuterium contained therein is isolated in Figure 4 in a view normal to the metal layers. The vertex Zr(2) atom closest to the viewer is seen to be displaced from the ideal threefold position to where it lies nearly over the Zr(2)–Zr(2) basal edge (3.525 Å), generating in this process two short (3.06-Å) and one long (3.90-Å) edge of the metal polyhedron. The shortest distance, 3.06 Å, is increased to 3.15 Å in the unoccupied chain of tetrahedra that share the 3.90-Å edge, attesting to the binding provided by deuteride in the former. The 3.90-Å distance must be virtually nonbonding, and therefore a better description of the environment about deuterium is in terms of a partially folded butterfly with a 3.90-Å distance between the wing tips. The deuterium is embedded within rather than bridging between the wing tips as the latter positioning would reduce its coordination number to two. There are no molecular analogues of the former configuration while the bridged examples show strong, $\pi$-bonding of the light atom (e.g., carbon) to the wing tips (iron),[20] which of course will not occur with deuterium. The larger and more distorted chains of tetrahedra that alternate with the points of the zigzag chain along *b* (Figure 2b) and remain unoccupied in this structure (at 14 K) have a more open butterfly configuration and are likely involved in the lower temperature hydrogen mobility mode that is observed in this compound by NMR starting at about 170 K.[9] The present results, especially the definition of the different types of potential hydrogen sites,

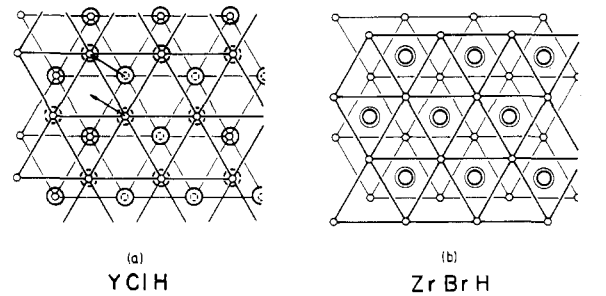


**Figure 5.** The structure of (a) $YClH_x$ ($TbClD_{0.8}$) (ccp, ZrBr type) and (b) ZrBrH (hcp) viewed normal to the layers: small circles, zirconium; large circles, hydrogen. Displacement of the top metal and hydrogen layers (plus bromine) according to the arrows in (a) converts the $YClH_x$ ($TbClD_{0.8}$) structure to that of ZrBrH (b) via the $Zr_2Br_2H$ intermediate (Figure 2b).

provide considerable support for the earlier NMR analysis.

The description of the transformation of either the ZrX or the ZrXD structures to this intermediate (below) includes the general distinction that the deuterium atoms virtually "follow" (remain bonded to) the triangular basal units rather than the single vertices of the tetrahedra during this process. This condition maximizes the distance between deuterium and its nearest-neighbor bromine atom (Figure 1). The deuterium is actually slightly displaced from the central position (Figure 4) with 2.03-Å distances to two basal Zr(2) atoms and 2.13 Å to the third (Zr(1)), this change bringing the deuterium closer to the more distant vertex Zr(2) at 2.20 Å. For comparison the Zr–H distances in $\delta$–$ZrH_{2-x}$ (fluorite) are 2.08 Å[21] while the threefold coordination of deuterium in ZrBrD occurs at 2.027 (1) Å.

It is not completely obvious why the zigzag chain ordering of deuterium should be preferred over the others. The layered arrangement in Figure 2c maximizes the D–D separation at ~3.4 Å vs. 2.20 Å in the ordered ZrBrD and 2.93 Å here, but this is accompanied by the formation of polar slab structure since only the upper or lower set of tetrahedral sites is occupied. The present hemideuteride structure does allow the formation of four strong Zr–D bonds with little decrease in Zr–Zr bonding; the interlayer separations of 3.13 Å (×3) in ZrBr are replaced by those at 3.06 (×2), 3.15, and 3.90 Å in the hemideuteride while the sixfold intralayer metal–metal distances show perhaps a small decrease. The small net increase in Zr–Zr distances on formation of $Zr_2Br_2D$ is also reflected in the fact that only 20% of the volume increase between ZrBr and ZrBrD occurs in the first step to the hemideuteride.[6] Interlayer metal–metal separations in ZrBrD are by comparison a relatively large 3.365 Å.

Another interesting possibility for a hemihydride structure would be half-occupancy of the tetrahedral sites in the ZrBr structure (Figure 1a). Although this would not produce a unique hemihydride composition without some distortion so as to differentiate the sites, such a structure is found with $YClH_x$ in a ZrBr structure type where $x$ is variable and near 0.6 at the lower limit. The Y–H distance inferred from an X-ray study is 2.23 Å at $x$ = 0.7, close to the sum of crystal radii.[11] The smaller size of the tetrahedra in ZrBr alone does not preclude hydrogen uptake ($d$(Zr–midpoint) = 2.05 Å)). Hydrogen in fact dissolves in ZrBr, presumably in the tetrahedral sites, to at least the composition $ZrBrH_{0.2}$ without any structural change evident to X-rays, but the phase appears to be metastable as it disproportionates to ZrBr and $Zr_2Br_2H$ above about 250 °C.[22] Instead, the reason for this contrasting behavior between YClH and ZrXH appears to be electronic, as will be considered shortly.

**Structural Interconversions.** The contrast between the ZrBr (YXH) and the ZrXH structures and the intermediacy of $Zr_2Br_2H$ are described approximately in Figure 1 in terms of their equivalent sections. The small dots therein represent hydrogen positions as

(20) Wijeyesekera, S. D.; Hoffmann, R.; Wilker, C. N. *Organometallics* **1984**, *3*, 962.

(21) Beck, R. L.; Mueller, W. M. In *Metal Hydrides*; Mueller, W. M., Blackledge, J. P., Libowitz, G. G., Eds.; Academic: New York, 1968; p 273.

(22) Marek, H. S.; Corbett, J. D., unpublished research.

defined in $YClH_{0.7}$[11] (and, better, in the comparable $TbClD_{0.8}$[13]), $Zr_2Br_2D$ (subcell), and ZrBrD.[10] The geometrical aspects of the interrelationship can be better visualized in a three-dimensional way with Figure 5 where two layers of the zirconium (small circles) and the two hydrogen layers between these (large circles) are illustrated for one slab of YClH (ZrBr type) (a) and ZrBrH (b). The hydrogen site symmetries, tetrahedral on the left and doubly occupied octahedral on the right, are more obvious in this way. The transition between these or to the intermediate $Zr_2Br_2H$ can be accomplished by displacing the top half, that is, the bromine (not shown, above and below octahedral interstices), metal, and hydrogen layers with respect to the bottom three layers, the hydrogen atoms thus remaining tied to the triangular faces of the adjoining metal layers. Displacement of the three layers in YClH as shown by the arrows in Figure 5a carries it into the ZrBrH structure, Figure 5b. The structure of $Zr_2Br_2H$ is achieved by stopping the process in either direction at the approximate midpoint so that each zirconium atom in the upper layer is almost directly above and bisects a zirconium–zirconium separation in the lower. The actual structure is just off this saddle point (Figure 2b and Figure 4). Of course, in either case half of the hydrogen is rejected by the lower symmetry of the intermediate structure. A related but less clear picture of the same thing involves the successive displacement of the top two layers plus hydrogen in part a or c of Figure 1 toward one another.

As noted before, strong zirconium–hydrogen covalent bonding must provide much of the driving force for the formation of these hydrides. The clear development of a filled hydride (plus zirconium) band analogous to that in $ZrH_2$ is seen in the helium I PES data of these phases. The spectra for $Zr_2Cl_2H$ and $Zr_2Br_2H$ show both are clearly metallic, and the same is probable but not certain for the ZrXH phases.[17] In fact, the virtually identical photoionization spectra seen for the conduction band of the two hemihydrides appear to assure that they have very similar structures.

**Electronic Effects.** Although all of the structural results already described obviously involve "electronic effects", there are some aspects that can be interpreted in relatively simple terms on the basis of the results of extended-Hückel band calculations.[23] These lie along the structural pathway YX–YXH–ZrXH (X = Cl, Br) and involve two questions: (1) why does YX not exist free of hydrogen and analogous to ZrX, and (2) why do the hydrogen site and the structural packing change so markedly on transition from YXH ($d^1$) to ZrXH ($d^2$)?

The first is relatively easy to account for: the density of states calculated for YCl exhibits a very high value at $E_F$ and, in addition, some Y–Y bonding states remain empty. The former condition is generally indicative of some sort of an instability, and the material is experimentally unstable with respect to metal plus $Y_2Cl_3$ when hydrogen is removed.[11] Intercalation with lithium in the absence of hydrogen does not move $E_F$ off of the peak sufficiently either, the system yielding LiCl and Y instead.[24]

The problem regarding the stability of MXH phases with cubic close packing of the heavy atoms and hydrogen presumably in tetrahedral holes such as YXH, $GdXH_x$, etc.[11,13,25] relative to those with hexagonal-close-packed layers and double hydrogen atoms in trigonal-antiprismatic interstices as in ZrXH is less obvious. There is substantial evidence that a rearrangement of the heavy atoms to hcp is necessary *if* the octahedral sites are to be singly occupied by boron, carbon, etc., since separation of the interstitial and the halogen atoms along *c* is otherwise too short (part a vs. part c of Figure 1).[10,26] This separation with a single hydrogen would be comfortably large, but double occupancy certainly requires the hcp arrangement. The answer to the second question has more to do with the instability of ZrXH in the cubic-close-packed structure with tetrahedral hydrogen. First, it should be noted that simple EHMO calculations reproduce the observation regarding stability. Figure 6 represents the calculated total energies of the tetrahedral structure (YClH) relative to those for the ZrBrD type for a rigid-band model and demonstrates that the tetrahedral arrangement is more stable with yttrium and other rare earths ($d^1$) than for zirconium ($d^2$) or the unknown niobium analogue ($d^3$). (The electron counts just used identify the population of the largely metal d conduction band per metal atom after the lower lying (and mainly) hydrogen and chlorine bands have been filled.[17]) In addition, Figure 6 shows that the effect does not depend on subtleties of hydrogen position within the somewhat compressed tetrahedral cavities.

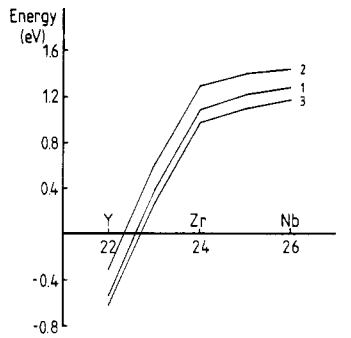


**Figure 6.** The total energy of the YClH structure (tetrahedral H) relative to that of ZrBrD type (doubly occupied octahedra) as a function of electron count in the cell (rigid band). The curves 1, 2, and 3 mark different positions of hydrogen within the tetrahedra.

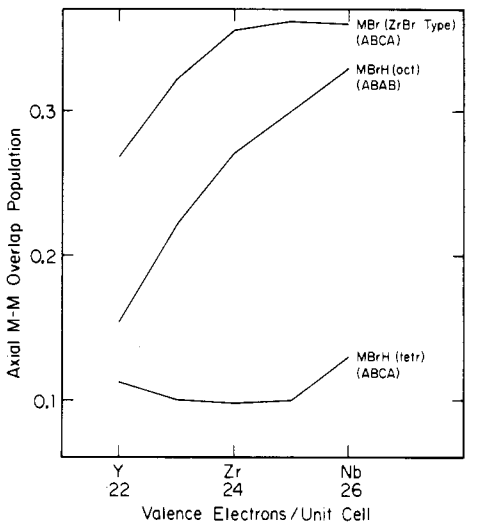


**Figure 7.** The metal–metal overlap populations between the double-metal layers for three structure types of a function of electron count in the series Y, Zr, Nb (rigid band): top, ZrBr type; middle, ZrBrD type; bottom, $YClH_x$ ($TbClD_{0.8}$) type.

Inspection of overlap populations for the states that are occupied between $d^1$ and $d^2$ allows the diagnosis of the principal source of this effect, the axial bonding between the two metal layers. The d–d overlap populations (proportional to bond strengths) for the interlayer M–M interactions summed over all occupied states are shown in Figure 7 as a function of electron count for the three different structure types. The bottom curve shows that there is actually a small decrease in the overlap population in the YBrH structure ($d^1$) on going from that compound to ZrBrH ($d^2$) (in a rigid structure and band). Thus, hydrogen in a tetrahedral site must interfere with the interlayer metal–metal bonding in that portion of the conduction band that is filled between $d^1$ and $d^2$. On the other hand, the hexagonal-close-packed (ZrBrH) version with pairs of hydrogen bonded in the larger trigonal-antiprismatic cavities, middle curve, shows a continued gain in metal–metal bonding as electrons are added in the transition from Y to Zr to Nb. This trend in bond strength also applies to the change from

(23) Hoffmann, R. *J. Chem. Phys.* **1963**, *39*, 1397.
(24) Meyer, G.; Hwu, S.-J.; Wijeyesekera, S. D.; Corbett, J. D. *Inorg. Chem.*, in press.
(25) Mattausch, Hj.; Schramm, W.; Eger, R.; Simon, A. *Z. Anorg. Allg. Chem.* **1985**, *530*, 43.
(26) Hwu, S.-J.; Ziebarth, R. P.; Winbush, S. v.; Ford, J. E.; Corbett, J. D. *Inorg. Chem.* **1986**, *25*, 283.

YBr to ZrBr in the parent ZrBr structure, top curve. Thus, it is not the structure type but the presence of hydrogen in tetrahedral cavities that is significantly destabilizing in the transition from YXH to ZrXH.

**Acknowledgment.** Dr. J. D. Jorgenson provided invaluable assistance in the collection of the two neutron diffraction data sets at Argonne National Laboratory. The writing of this paper took place while J.D.C. was on leave at the Institut für Anorganische und Analytische Chemie, Justus-Liebig-Universität, Giessen, West Germany, under the auspices of the Alexander von Humboldt-Stiftung, Bonn, BRD. J.D.C. is indebted to Professor R. Hoppe and Dr. G. Meyer for many considerations in this regard.

---

Contribution No. 4134 from the Central Research and Development Department, Experimental Station, E. I. du Pont de Nemours & Company, Inc., Wilmington, Delaware 19898

# A Cobalt Oxygen Carrier in Zeolite Y. A Molecular "Ship in a Bottle"

Norman Herron

*Received July 20, 1986*

Cobalt(II) ion exchanged zeolite Y has been treated with a flexible Schiff base ligand, SALEN, so as to synthesize the Co(II) complex inside the pore structure of the zeolite itself. Such a complex is rigid and of such a size that it is physically entrapped inside the zeolite pores. The complex, as its pyridine adduct, shows affinity for dioxygen and forms 1:1 adducts. The $O_2$ binding equilibria are less favorable while the adducts show excellent resistance to autoxidation even at elevated temperatures. The oxygen adduct forms at a rate limited by diffusion of the oxygen into the zeolite and with a binding constant similar to the same species in solution. Hill plots of the oxygen binding behavior at four temperatures show slopes of 0.56, indicating a negative cooperativity between the cobalt binding sites. This behavior is interpreted as the superposition of the oxygen sorption behavior of the zeolite itself upon the sorption behavior of the complex. Apparent thermodynamics of binding show $\Delta H = -11.4$ kcal/mol and $\Delta S = -51$ eu. Attempts to prepare the same complex in the smaller pore zeolite 5A lead only to a selective removal of cobalt ions from the exterior surface of the zeolite crystallites.

While we are all familiar with reactions in mini- and microglassware, consider the extrapolation of the reaction vessel dimensions to its logical minimum. Eventually the vessel size becomes similar to the molecular size of the materials being prepared. At this level a new set of chemistries may be imposed on the reactants merely by the physical limitations of the vessel inside which such chemistry is constrained to occur. Such is the domain of intrazeolite chemistry where chambers and channels of molecular dimensions provide the rigid aluminosilicate framework within which reaction chemistry may be performed. Mobil's methanol to gasoline process is one example of the modified reactivity that results from constraining chemistry to occur inside such small vessels.[1a] We have shown selectivities approaching 50:1 in the selective hydrogenation of mixtures of cyclopentene and 4-methylcyclohexene using rhodium-containing zeolites.[1b] We now seek to demonstrate a relatively new idea in intrazeolite chemistry relating to supported metal catalyst species, namely, that a metal complex prepared inside a zeolite can have substantially different reactivity than its solution analogue.[2] We have prepared a complex where all of the individual components (metal ion plus various ligands) may easily pass in and out of the zeolite, but the final assembled coordination complex is too large and rigid to pass out once assembled inside.[3] The fundamental questions of how such entrapped "ship in a bottle" species[4] behave as compared to the identical species in free solution is a fascinating problem related to the variation of both structural and reaction chemistry with scale. We now report a preliminary study of the synthesis and oxygen binding behavior of a cobalt Schiff-base complex inside zeolite Y as compared to the behavior of the same material in free solution. While there are previous reports of oxygen-carrying species inside zeolites, these are all ionic species that are not true encapsulated complexes, and in most instances they have no solution phase equivalents for comparison.[5]

## Experimental Section

Cobalt(II) ion exchange of zeolites CaNa-A (5A) and Na-Y (LZY-52) was carried out by following standard procedures.[6] A 10-g sample of zeolite in 1 L of distilled water was stirred with 0.2 g of cobaltous acetate at pH 6.5 for 4 h at 90 °C. The slurry was filtered and suction dried to give a pale pink powder, which, after being dried in a flow of dry oxygen at 400 °C, gives a blue purple solid with about one Co ion per eight supercages of the zeolite. These dried materials were treated with excess Schiff base ligand SALEN (1,6-bis(2-hydroxyphenyl)-2,5-diaza-1,5-hexadiene) (I) in an inert-atmosphere glovebox. This ligand

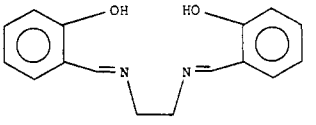


SALEN I

possesses two ionizable protons that are lost during complexation to a metal ion; thus, coordination to a divalent cation will result in the production of an electrically neutral complex and the liberation of two protons. Inside a zeolite, therefore, the released protons would become the charge compensators of the anionic zeolite framework, replacing the divalent metal ion in this capacity. The intimate mixtures of solids were heated to 120 °C for 30 min with continuous mixing during which time a yellow orange color developed. After cooling, the samples were Soxhlet-extracted with methylene chloride for 16 h in the inert atmosphere during which excess ligand and cobalt complex on the exterior of the zeolite crystallites were removed. The products were dried in vacuo at room temperature for at least 8 h and stored in the inert atmosphere. The samples were colored deep orange (zeolite Y) and blue (zeolite A).

Characterization of samples revealed the following: Chemical analysis of the zeolite Y sample shows between a 50% and 100% excess of the Schiff base ligand over the amount necessary to convert all of the cobalt to the complex. With zeolite A, essentially no ligand was detected by

(1) (a) Weisz, P. B. *Pure Appl. Chem.* **1980**, *52*, 2091. Smith, K. W.; Starr, W. C.; Chen, N. Y. *Oil Gas J.* **1980**, *78*(21), 75. (b) Corbin, D. R.; Seidel, W. C.; Abrams, L.; Herron, N.; Stucky, G. D.; Tolman, C. A. *Inorg. Chem.* **1985**, *24*, 1800.

(2) Camara, M. J.; Lunsford, J. H. *Inorg. Chem.* **1983**, *22*, 2498. Basset, J. M.; Theolier, A.; Commereuc, D.; Chauvin, Y. *J. Organomet. Chem.* **1985**, *279*, 147.

(3) Romanovsky, B. V. *Proc. Int. Symp. Zeolites Catal.* **1985**, 215. Meyer, G.; Wohrle, D.; Mohl, M.; Schulz-Ekloff, G. *Zeolites* **1984**, *4*, 80.

(4) This term was first used to describe $Ni(CO)_{n-4}L_n$ complexes entrapped in zeolite X. Herron, N.; Stucky, G. D.; Tolman, C. A. *Inorg. Chim. Acta* **1985**, *100*, 135.

(5) Howe, R. F.; Lunsford, J. H. *J. Am. Chem. Soc.* **1975**, *97*, 5156. Howe, R. F.; Lunsford, J. H. *J. Phys. Chem.* **1975**, *79*, 1836. Schoonheydt, R. A.; Pelgrims, J. *J. Chem. Soc., Dalton Trans.* **1981**, 914. Winscom, C. J.; Lubitz, W.; Diegruber, H.; Moseler, R. *Stud. Surf. Sci. Catal.* **1982**, *12*, 14.

(6) Schoonheydt, R. A.; Van Wouke, D.; Vanhove, M. *J. Colloid Interface Sci.* **1981**, *83*, 279.

0020-1669/86/1325-4714$01.50/0 